Title
A Hybrid Compliant—Tendon Laparoscopic Instrument for Distal Articulation and Grasping: Design and Experimental Validation

Journal
International Journal of Medical Robotics and Computer Assisted Surgery, 22(4)

ISSN
1478-5951

Authors
Kumar, Prabhat
Ravi, Bhallamudi

Publication Date
2026-08-01

DOI
10.1002/rcs.70206

A Hybrid Compliant–Tendon Laparoscopic Instrument for Distal Articulation and Grasping: Design and Experimental Validation

Prabhat Kumar (corresponding author)
Department of Neurological Surgery, University of California, San Francisco, USA
Mechanical Engineering Department
Indian Institute of Technology, Bombay, India
E-mail: prabhat.kumar@ucsf.edu

Bhallamudi Ravi
Mechanical Engineering Department
Indian Institute of Technology, Bombay, India
E-mail: prof.b.ravi@gmail.com

Data Availability Statement: The data that support the findings of this study are available on request from the corresponding author. The data is not publicly available due to privacy or ethical restrictions.

Funding Statement: This research did not receive any specific grant from funding agencies in the public, commercial, or not-for-profit sectors.

Conflict of Interest Disclosure: The authors declare that they have no competing interests.

Human participants and/or animals: This article does not contain any studies with human and/or animal participants performed by any of the authors.

Author Contributions
Prabhat Kumar: Conceptualization, Data curation, Formal analysis, Investigation, Methodology, Software, Validation, Visualization, Writing – original draft, Writing – review & editing.
Bhallamudi Ravi: Conceptualization, Investigation, Supervision, Writing – review & editing

Abstract

Background: Conventional laparoscopic instruments provide limited dexterity in confined anatomical environments, while existing articulated designs rely on complex rigid joints or motorized actuation, increasing mechanical complexity and limiting miniaturization.

Methods: A hybrid compliant–tendon laparoscopic instrument was developed to integrate articulated distal motion and active grasping within a 5 mm form factor. The compliant segment was fabricated from super-elastic Nitinol, and grasping was achieved using a tendon–pulley mechanism. The system was evaluated using nonlinear finite element analysis and experimental testing, including digital image correlation and benchtop force measurements.

Results: The mechanism achieved up to 75° articulation with mean model errors below 8%. The grasper produced a maximum force of 13.2 ± 0.47 N and maintained performance across articulation angles. Pull-out tests confirmed stable interaction with soft-tissue analogs.

Conclusions: The proposed design demonstrates a compact, low-complexity approach for combining compliant articulation and tendon-driven grasping within a 5 mm surgical instrument.

Keywords: *Minimally invasive surgery; Laparoscopic instruments; Surgical robotics; Compliant mechanisms; Tendon-driven systems; Articulated instruments*

1. INTRODUCTION

Minimally invasive surgery (MIS) has transformed modern surgical practice by reducing patient trauma, postoperative pain, and recovery time. However, these benefits are often limited by the dexterity constraints of conventional laparoscopic instruments, which typically provide only four degrees of freedom and restrict the surgeon's ability to perform complex tasks in confined anatomical spaces. Procedures such as suturing, dissection, and triangulation require enhanced distal articulation and precise manipulation, which remain challenging with standard rigid instruments.

To address these limitations, articulated laparoscopic instruments and robotic systems have been developed to improve dexterity at the instrument tip. While robotic platforms offer advanced motion capabilities, they often involve high cost, complex actuation systems, and maintenance requirements. Handheld articulated instruments provide a more accessible alternative; however, existing designs typically rely on rigid-link mechanisms or tendon-driven systems that introduce trade-offs between mechanical complexity, force transmission efficiency, and miniaturization.

1.1. Rigid-Body-based Articulating (RBA) Mechanisms

RBA mechanisms are based on discrete links and revolute joints arranged in serial or parallel mechanisms. Their advantages include predictable kinematics, high stiffness, and robust force transmission. Instruments like the RealHand (Novare Surgical) and da Vinci EndoWrist (Intuitive Surgical) leverage these mechanisms to provide 7-DOF intracorporeal dexterity [3]. Similarly, Kumar et al. presented a novel 7-DOF instrument using only rigid links to enhance reusability and affordability [4]. Despite their widespread clinical use, rigid-link instruments are complex, often requiring dozens of precision components, bearings, and pins. This increases instrument weight, cost, and susceptibility to mechanical wear, backlash, and alignment issues [5]. Sterilization and cleaning are further complicated by multiple moving parts, making them less desirable for disposable or resource-limited surgical settings.

1.2. Cable-Pulley-based Articulating (CPA) Mechanisms

CPA mechanisms use flexible cables (or tendons) routed through the instrument shaft to transmit motion from a proximal handle to the distal tip. This design enables compact packaging and higher DOF in long, slender devices. Robotic systems such as the da Vinci surgical system utilize this mechanism to great effect, allowing intuitive, tremor-filtered manipulation of end effectors. Further innovations in this area include tendon-driven mechanisms with detachable end-effectors, aiming to improve modularity and ease of sterilization. However, these systems are prone to nonlinear behaviors due to cable stretch, slack, friction, and cumulative hysteresis, particularly under repeated load cycles. Backlash-induced errors can degrade control fidelity, especially in tasks requiring sub-millimeter precision such as suturing or vascular dissection. Furthermore, cable routing often requires large curvature radii, limiting miniaturization and increasing assembly complexity [6].

1.3. Compliant Mechanisms

Compliant mechanisms are monolithic structures that achieve motion through elastic deformation of flexible segments rather than discrete joints. This eliminates moving parts, reducing friction, wear, and the need for lubrication. These mechanisms are lightweight, sterilizable, and amenable to microfabrication, making them well-suited for disposable or miniaturized MIS instruments. Materials such as Polyether Ether Ketone (PEEK), Polyimide, or super-elastic Nitinol have been used to realize compliant devices that exhibit recoverable deformation over large strains [7].

In MIS, compliant mechanisms have been employed in graspers, steerable catheters, and articulated forceps. Notably, Hong and Jo demonstrated a 2-DOF compliant forceps with integrated force sensing using flexure hinges [8]. Chandrasekaran and Thondiyath developed a tether-driven minimally invasive robotic surgical tool with a decoupled degree-of-freedom wrist, demonstrating the feasibility of separating actuation pathways to improve dexterity in confined surgical environments [9]. Venkiteswaran et al. proposed a notch-based compliant wrist segment made of Nitinol, enabling deflections up to 90° [10].

Despite these advances, achieving both large articulation and sufficient load-bearing capability within a compact laparoscopic form factor remains a significant challenge. Many compliant designs either prioritize deformation capability at the expense of force transmission or focus on grasping without integrating multi-DOF articulation. As a result, the simultaneous realization of dexterity, force capability, and miniaturization remains limited in existing systems. While decoupled tendon-driven mechanisms have been explored in robotic surgical tools [9], integration of articulated compliant motion and load-bearing grasping within a 5 mm laparoscopic instrument remains comparatively unexplored.

In parallel, commercially available articulated laparoscopic instruments, such as EndoWrist (Intuitive Surgical), RealHand (Novare Surgical), ArtiSential (LivsMed), and FlexDex, provide enhanced dexterity but rely on rigid-link joints, cable–pulley transmissions, or motorized actuation (Table i). These approaches often introduce increased mechanical complexity, higher cost, and challenges in sterilization and maintenance, particularly for compact or disposable instruments [4].

Overall, articulating mechanisms exhibit a fundamental trade-off between articulation capability, force transmission, and mechanical complexity. Rigid-body mechanisms provide predictable kinematics and high stiffness but require complex assemblies with multiple joints, increasing cost and sterilization burden. Cable–pulley systems enable compact multi-DOF articulation but introduce nonlinearities such as friction, slack, and hysteresis, which degrade control fidelity and force transmission. Fully compliant mechanisms eliminate discrete joints and simplify fabrication; however, they are limited either to micro-scale manipulation with low load-bearing capability or to macro-scale flexure-based designs that do not integrate high-force grasping.

These limitations define a design gap for a compact, manufacturable mechanism that can simultaneously achieve large articulation, sufficient load-bearing grasping force, and reduced mechanical complexity. To address this challenge, our prior work developed and validated a compliant articulating segment using topology optimization, rigid-body replacement, and pseudo-rigid-body modeling (PRBM) [14]. The mechanism achieved up to 80° of articulation within a 5 mm instrument diameter and was validated through nonlinear finite element analysis. Building upon that foundation, the present work introduces a hybrid compliant–tendon mechanism that integrates distal articulation and active gripping within a compact laparoscopic architecture. In contrast to fully rigid wrist mechanisms that depend on multiple joints and complex assemblies, and unlike fully compliant end-effectors that often experience reduced load-bearing capacity, the proposed mechanism functionally separates articulation and force transmission. Compliance is confined to the distal wrist segment to enable large-angle deflection without joints, while grasping force is generated through a tendon–pulley transmission optimized for force amplification.

Table i: Comparison of commercially available articulating laparoscopic instruments. [2], [15]

Device (Manufacturer)	Mechanism Type	Actuation Method	Distal DOF (Pitch / Yaw / Roll / Jaws)	Max Articulation Angle	Key Limitations	Market Status
EndoWrist (Intuitive Surgical)	Rigid body based	Tendon-driven robotic actuators	3 DOF wrist + jaw actuation	~90° pitch & yaw	Limited uses, expensive, complex sterilization	Commercial (global)
ArtiSential (LivsMed)	Cable and pulley-based	Cable-driven ergonomic handle	360° rotation + pitch, yaw + jaws	>90° multidirectional	Stiff learning curve; increased handle bulk	Commercial (US, EU, South Korea)
FlexDex (FlexDex Surgical)	Cable- and pulley-based	Forearm-controlled mechanical mapping	3 DOF wrist + jaws	~90°	Only needle holder is available, no tremor filtration	Commercial (US & EU)
Kymerax (Terumo)	Motor-assisted handheld articulation	Onboard micro-motors drive wrist joints	Multi-DOF	>90°	Requires powered console; heavy handle	Commercial (CE-approved, Europe/Asia)
RealHand (Novare Surgical)	Rigid body based	Pure mechanical mirroring of surgeon's wrist	7 DOF (Pitch–yaw mimicking user's wrist + jaws)	~80°–90°	Lower mechanical advantage, fatigue at joints	Commercial (discontinued development)
Radius Surgical System (Tuebingen Scientific)	Rigid body based	Handle-controlled mechanical articulation + thumb-knob rotation	Deflection + rotation (2 added DOF)	~80° deflection; 360° rotation	No motion scaling; limited jaw force options	Commercial (FDA-cleared, reusable)
HandX Surgical System (Human Xtensions)	Cable and pulley-based	Motorized distal articulation + motion scaling	Multi-DOF wrist + jaws	~70°–90°	Electronics maintenance; cost	Commercial (FDA-cleared)
JAiMY / JAiMY Advance	Cable and pulley-based	Full wrist + jaw actuation	Electric motor drive + handheld controller	~90°	Limited device set (needle driver primary)	Commercial (EU), limited markets

The primary contribution of this work is the compact integration and experimental validation of a compliant articulating segment and a tendon-driven gripper within a 5 mm laparoscopic instrument. Building upon prior studies of compliant articulation and decoupled tendon-driven surgical tools [9,14], the present work demonstrates that large-angle articulation and load-bearing grasping can be combined within a miniaturized form factor. In addition, DIC-assisted measurements and nonlinear FEA are used to quantitatively validate the mechanical performance of both the compliant segment and the integrated prototype.

2. MATERIALS & METHODS

The present study follows a multi-stage approach to the design, integration, and validation of a compliant mechanism-based articulating laparoscopy device. Building upon prior work on compliant articulation, developed using nonlinear FEA and PRBM, this study extends the existing mechanical framework [14]. Specifically, it introduces a cable-based gripper, integrates it with the compliant wrist segment, and validates the complete laparoscopy instrument through experimental testing.

In the prior work, the compliant wrist segment was synthesized using a strain energy-based topology optimization framework, followed by dimensional refinement under nonlinear finite element analysis (FEA). The large-deflection behavior of the compliant segment was modeled using a pseudo-rigid-body model (PRBM), in which the flexible beam was represented by equivalent rigid links connected via torsional springs located at characteristic pivots ($\gamma = 0.85$).

The torsional stiffness *(K)* was defined as,

$$K = \frac{2\gamma k_\theta EI}{l} \ldots (i)$$

enabling derivation of closed-form kinematic and force–deflection relationships, where E is the Modulus of elasticity of the material and I is the Area Moment of Inertia. The articulation angle was analytically related to actuator displacement, while the required input force was expressed as a function of bending stiffness $(k_\theta)$and articulation angle (θ). Nonlinear FEA incorporating geometric and material nonlinearities (superelastic Nitinol model) was used to validate strain limits and range-of-motion predictions. Detailed derivations and optimization methodology are reported in [14].

Guided by this validated compliant articulation framework, the present study focuses on integration and device-level performance. The design was governed by the following functional requirements, adopted from prior analyses of laparoscopy instruments [16]:

i. Achieve a minimum grasping force of 10 N to securely manipulate soft tissue.
ii. Fit within the 5 mm outer diameter constraint of standard laparoscopic trocars.
iii. Enable articulated distal motion together with independent grasping functionality.
iv. Ensure reusability through elastic deformation within safe operational strain limits.

Based on these design constraints and requirements, the overall architecture and working principle of the proposed instrument were established as described below.

1.1. Ethics Statement

The current study involved the design and benchtop evaluation of a mechanical device and did not involve human participants, animal experiments, or patient data. Therefore, ethical approval and informed consent were not required.

1.2. Device Design and Working Principle

To improve clarity and reproducibility of the proposed mechanism, a system-level kinematic and actuation schematic is presented in Figure i. The figure illustrates the complete mechanical architecture, including the compliant articulation segment, push–pull rod actuation, tendon routing, and distal force transmission. This representation provides a direct visualization of the functional interaction between articulation and grasping mechanisms.

The proposed laparoscopic instrument integrates three primary subsystems to achieve high-dexterity manipulation:

i. A distal compliant articulation segment fabricated from super-elastic Nitinol,
ii. A tendon–pulley-driven gripper mechanism, and
iii. Proximal actuation inputs.

The mechanism operates through two decoupled actuation pathways. Articulation is achieved by differential displacement of push–pull rods, which induces elastic bending of the monolithic compliant wrist segment. Grasping is achieved through a tendon–pulley mechanism, where tendon displacement (Δs) produces jaw rotation (α) through a distal pulley of radius R_p, generating gripping force (F_g) via the jaw lever geometry.

This functional separation of articulation and force transmission enables simultaneous articulation and grasping with minimal mechanical interference. Following the establishment of the articulation mechanism, the gripper subsystem was designed to meet the required force transmission and structural constraints.

For the purposes of experimental validation, the present study focuses on a single-plane articulation mode of the compliant segment together with independent grasping functionality. While the articulated segment can be oriented in different spatial planes through rotation of the instrument shaft, independent multi-axis articulation and coupled three-dimensional motion were not investigated in the present study.

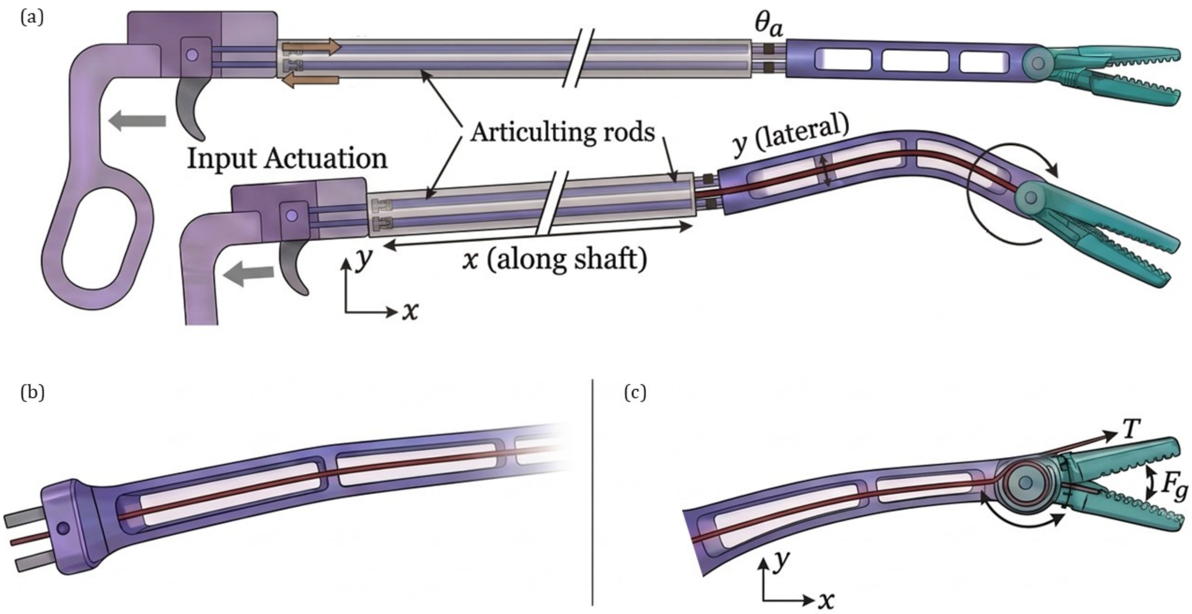

Figure i: Kinematic and actuation schematic of the proposed hybrid compliant–tendon mechanism. (a) System-level view showing push–pull rod actuation for articulation and tendon-driven grasping; (b) *deformation of the compliant segment under actuation; (c) distal force transmission illustrating tendon-driven jaw rotation and gripping force. The tendon is routed along the compliant segment, enabling simultaneous articulation (θ_a) and grasping (F_g) with minimal kinematic coupling.*

1.2.1. Force Transmission Model of the Gripper

To provide a first-order analytical description of the gripper subsystem, a quasi-static force-transmission model was developed relating tendon displacement, tendon tension, and resulting gripping force.

The tendon-driven gripper converts tendon displacement into jaw rotation through a pulley mechanism. Assuming negligible tendon stretch, the angular rotation of the jaw, α, can be expressed as,

$$\alpha = \frac{\Delta s}{Rp} \ldots (ii)$$

where (Δs) is the tendon displacement and (R_p) is the effective pulley radius.

Under quasi-static conditions, the tendon tension (T) generates an input moment about the jaw pivot given by,

$$M_{¿} = T \bullet L_{¿} \ldots (iii)$$

where L_{in} is the effective tendon moment arm.

The gripping force (F_g) is generated at the jaw tip through the corresponding output lever arm (L_{out}). Equating the input and output moments,

$$T \bullet L_{¿} = F_g \bullet L_{out} \ldots (iv)$$

Rearranging Eq. (iv) gives

$$F_g = T \frac{L_{¿}}{L_{out}} \ldots (v)$$

Equation (v) indicates that the gripping force is directly proportional to tendon tension and is amplified by the geometric lever ratio of the jaw mechanism.

During articulation, the tendon follows a curved routing path through the compliant segment. This introduces articulation-dependent transmission losses, resulting in a reduction of the effective gripping force. To characterize the articulation-dependent reduction in force transmission, a transmission-efficiency parameter (η) is defined as,

$$\eta = \frac{F_{g,\theta}}{F_{g,0}} \ldots (vi)$$

where ($F_{g,0}$) is the gripping force at the neutral configuration and ($F_{g,\theta}$) is the gripping force at articulation angle (θ).

Accordingly,

$$F_{g,\theta} = \eta(\theta) F_{g,0} = \eta(\theta) \cdot T \frac{L_{¿}}{L_{out}} \dots (vii)$$

This formulation provides a first-order analytical framework linking tendon displacement, tendon tension, jaw kinematics, and gripping force within the hybrid compliant–tendon mechanism. It also enables interpretation of the experimentally observed variation in gripping force with articulation angle. The model is intentionally simplified and is intended to describe the dominant kinematic and force-transmission relationships within the mechanism. Distributed tendon friction, local contact effects, and geometric nonlinearities are not explicitly modeled; instead, their combined influence is represented through the transmission-efficiency parameter η. The value of η is subsequently determined experimentally in Section 3.4.3 through measurements of gripping force at different articulation angles.

1.3. Gripper Design and Structural Analysis

Laparoscopic procedures employ a variety of instruments, including graspers, forceps, dissectors, and bipolar or monopolar devices. Among these, graspers are reported to experience the highest operational loads, second only to staplers [18]; accordingly, a grasper was selected as the end-effector for development in this study. Based on the functional requirements outlined above, the gripper was required to generate a minimum grasping force of 10 N [4]. The jaw dimensions and pulley radius were selected to achieve the required grasping force while limiting tendon tension to practical actuation levels and ensuring structural safety under FEA-verified stress limits. The geometric lever ratio of the jaw was chosen to provide sufficient force amplification within the distal 5 mm form factor.

Multiple gripper mechanisms can potentially satisfy this requirement; however, their suitability depends on trade-offs among articulation capability, mechanical complexity, force transmission efficiency, and size. To systematically evaluate these trade-offs, three commonly adopted mechanisms were shortlisted: a rigid-body linkage mechanism, a single-tendon gripper, and a two-layered pulley system. These candidates were assessed to identify the most appropriate configuration for integration with the compliant articulating wrist. Although rigid-body linkage mechanisms offer high force amplification, their complexity and limited scalability to a 5 mm form factor restrict their applicability for highly articulated designs.

1.3.1. Evaluation *of Design Options*

After the various types of mechanisms were considered along with their advantages and disadvantages, a matrix evaluation table was prepared based on the following criteria:

i. Coupling of grippers with high articulation: The gripper should be able to open and close while the wrist is articulated at higher angles (say, articulations of more than 45°).
ii. Complexity of the mechanism: The gripping mechanism should be designed in such a way that it achieves the desired function with a minimal number of parts.
iii. Grasping force: The gripper should be able to withstand as well as exert a sufficient amount of force to hold the tissues.
iv. Size and manufacturability: The gripper needs to be compact enough to fit through the natural orifice of the human.

Each mechanism was scored using a five-point ordinal scale (1–5), where higher values indicate better performance relative to the functional requirements. The total score (maximum = 20) was used to rank the candidate mechanisms. The results, summarized in Table ii, indicate that while the rigid-body mechanism exhibited high force transmission, it was penalized by size and articulation limitations. The single-tendon design offered compactness and simplicity but provided insufficient gripping force. The two-layered pulley mechanism achieved the highest overall score, balancing articulation capability, force efficiency, and compactness, and was therefore selected for further development and validation.

Table ii: Matrix evaluation of the various mechanisms for the gripper

Gripper mechanism	Articulation	Complexity	Force	Size	Total
Rigid-body based	2	2	5	1	10
Single tendon gripper	4	4	2	4	14
Two-layered pulley	4	4	4	3	15

Since significant stress concentrations may arise in gripper jaws during tissue grasping, exceeding material yield limits would result in permanent deformation and functional failure. Accordingly, nonlinear FEA was performed to verify the structural integrity of the selected design.

1.3.2. Non-*Linear FEA of Gripper*

During laparoscopic use, the gripper jaws were analyzed under critical loading conditions representative of surgical grasping. The jaws were modeled as a cantilever beam with the hinge region defined as the fixed support. A load of 15 N, consistent with ISO 9711-1 standards for laparoscopic instruments, was applied at the jaw tip, while the proximal face was fully constrained. Figure ii illustrates the loading and boundary conditions. The gripper assembly consisted of tungsten carbide jaws silver-brazed to a stainless-steel (SS316L) base to ensure adequate structural strength. This configuration was reproduced in Ansys Workbench by assigning appropriate material properties and defining a bonded contact at the brazed interface to represent the rigid connection between dissimilar materials.

The structural analysis was performed under quasi-static conditions, treating the SS316L grasper as a linear elastic material. Idealized boundary conditions were applied to represent worst-case loading conditions at the hinge and jaw tip. These modeling assumptions are consistent with static strength verification of miniature metallic mechanisms. The simulation enabled evaluation of stress distribution and deformation under peak loading conditions to confirm structural safety and functional reliability.

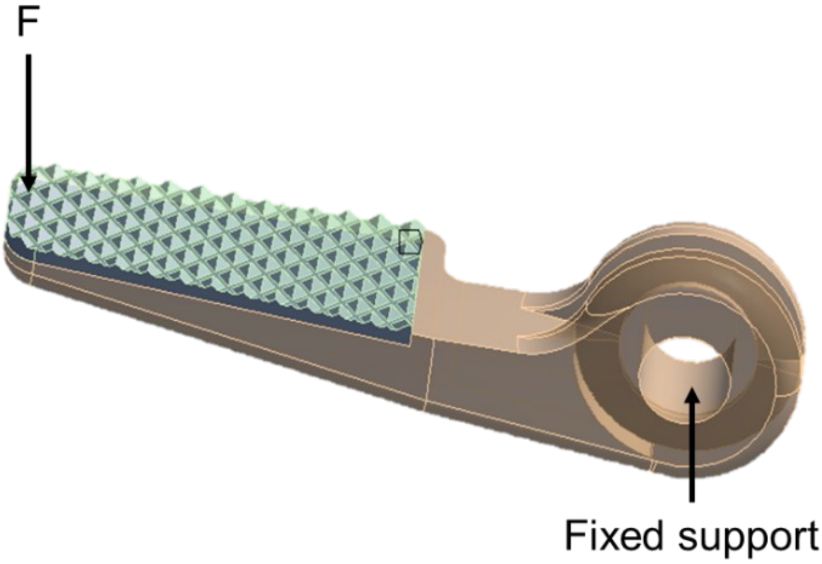

Figure ii: Finite element analysis setup of the gripper showing the applied load at the jaw tip and fixed boundary condition at the hinge.

1.3.3. Mesh Convergence *Study*

To ensure the accuracy of the FEA model while maintaining computational efficiency, a mesh convergence analysis was conducted in Ansys Workbench. The mesh size was progressively refined from 0.40 mm to 0.20 mm in increments of 0.02 mm. The convergence criterion was based on the stabilization of maximum von Mises stress values. Convergence was achieved at a mesh element size of approximately 0.26 mm, beyond which further refinement produced negligible changes in stress (<2%) but increased computational time largely. Therefore, a mesh size of 0.26 mm was selected for subsequent analyses as the optimal balance between accuracy and efficiency.

1.3.4. Results and Analysis

With the optimal mesh established, a 15 N load was applied at the gripper tip to simulate peak surgical loading. Owing to geometric variation along the jaw length, the maximum stress did not occur at the tip but in the transition region near the hinge. The nonlinear FEA results showed a maximum von Mises stress of approximately 200 MPa, which is well below the yield strength of tungsten carbide ($\approx$ 350 MPa), indicating that the design is structurally safe under operational conditions (Figure iii).

Stress concentration regions (with a max. stress of around 200 MPa) were observed primarily at the inner corners near the hinge and at the neck where the cross-section changes abruptly. These local effects can be mitigated by filleting internal corners, smoothing geometric transitions, and minimizing material removal in critical load-bearing areas. Overall, the FEA confirmed that the gripper design satisfies the strength and deformation requirements for laparoscopic grasping applications.

1.4. Prototype Fabrication and Experimental Setup

The validated gripper design was fabricated to experimentally verify the FEA predictions. The simulated 15 N load corresponds to suspending approximately 1.53 kg at the gripper tip;

although such forces are uncommon in clinical use, they provide a conservative design margin. Minor dimensional refinements were implemented to reduce localized stress concentrations and improve manufacturability.

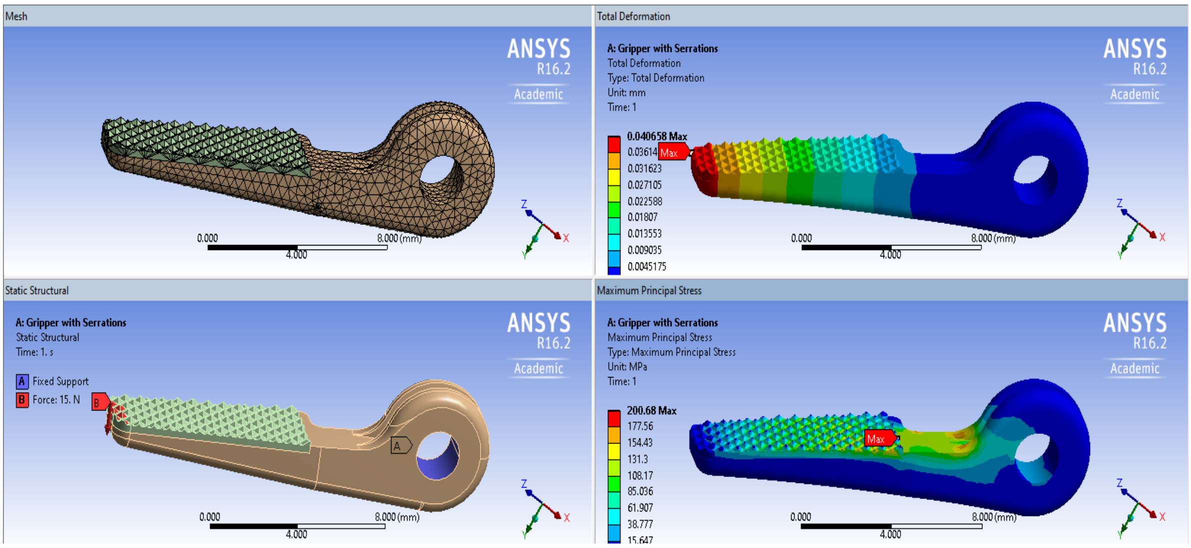

Figure iii:FEA results of the gripper

Two fabrication approaches were evaluated: metal additive manufacturing and wire electrical discharge machining (Wire-EDM). Although the additively manufactured prototype exhibited adequate geometric fidelity, it lacked the sharp jaw edges required for effective tissue grasping. Consequently, the Wire-EDM–fabricated prototype was selected for all subsequent testing (Figure iv (a)).

The complete instrument assembly comprised grasper jaws, a compliant articulation mechanism, actuation rods, tendon-driven grasper actuation, tendon guides, and alignment components (Figure iv (b)). The compliant articulation segment was fabricated from super-elastic Nitinol (SE508), while the grasper was machined from SS316L. Ti–6Al–4V rods were used for actuation and laser-welded to the compliant mechanism. Tendon actuation was implemented using 1×7 strand stainless-steel (SS304) cables of 0.5 mm diameter, selected for their flexibility, tensile strength, and availability at small diameters. A safety factor of 10 was applied when estimating allowable tendon loads, consistent with prior tendon-driven instrument studies [19].

SS304 tendon aligners, fabricated by EDM drilling of 3 mm thick disks, were used to maintain tendon alignment along the curved shaft. A flexible, 3D-printed tendon guide ensured consistent routing and was connected distally to the articulation mechanism and proximally to the outer pipe. Tendon ends were crimped using aluminum sleeves to prevent slippage during repeated actuation cycles. Interference analysis in SolidWorks confirmed appropriate clearances prior to assembly. All geometric selections were constrained by the 5 mm outer diameter requirement and internal routing space necessary for actuation shafts and tendons.

Following fabrication and assembly, the prototype, comprising the compliant articulation and integrated grasper, was prepared for experimental validation. Validation was performed in two stages: first, characterization of the compliant articulation segment alone, and second,

evaluation of the fully integrated instrument. The following section presents experimental procedures and results.

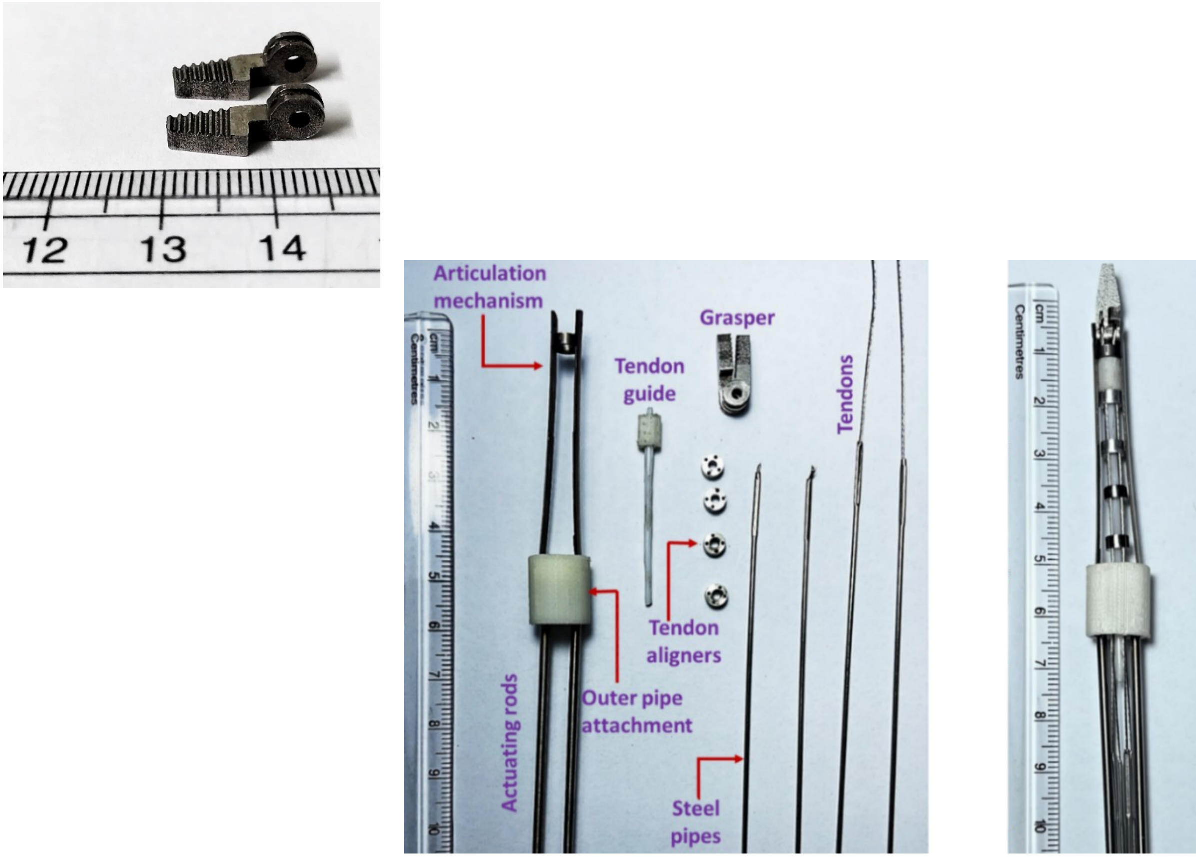

(a) *(b)*

Figure iv:(a) Gripper prototype fabricated using metal 3D printing (top) and wire-EDM (bottom), (b) Assembly of the instrument along with components

3. RESULTS

The performance of the compliant articulation mechanism and the fully assembled hybrid instrument was evaluated through a series of benchtop experiments. The validation process consisted of two stages: (i) characterization of the compliant articulation segment to assess angular deflection, repeatability, and motion accuracy, and (ii) testing of the integrated system to quantify grasping forces, articulation capabilities, and mechanical response under representative surgical conditions.

A set of experiments was conducted to characterize the free articulation of the compliant structure. For this purpose, a dedicated benchtop test setup was fabricated. The experiments were conducted on a Planar Biaxial Testing System, and deflection measurements were obtained using a Digital Image Correlation (DIC) camera to enable high-accuracy, full-field displacement analysis. The experimental configuration allowed for precise actuation control and visual tracking of the articulating segment's deformation under incremental tendon displacements. These measurements were compared directly with the simulated response from the FEA model to assess correlation and identify potential nonlinear effects not captured computationally.

1.1. Design and Fabrication of Test Setup

To mechanically verify the feasibility of the proposed mechanism, a series of tests were conducted on articulation and under loading/unloading conditions. The mechanism was designed such that the articulation is in the range of 80° - 90°. Since the compliant mechanism inputs are displaced in opposite directions, a test setup capable of applying colinear but opposing displacements was required. The entire setup was fabricated in Aluminium material using wire-EDM and drilling processes. Sliders were used for carrying out the displacement motion. The fixed base was clamped on the planar bi-axial testing system, while the actuation rods were secured by the jaws. As the jaws applied opposing displacements, a DIC camera started capturing the images of the end-effector (Figure v). The details of the Planar biaxial system and the DIC camera are presented below.

1.2. Instrumentation Details

Planar Biaxial Testing System (MTS Systems Corp., USA): The planar biaxial machine applies and measures in-plane forces along both X and Y axes using servo-hydraulic actuation. Each of its four actuators provides up to 100 kN load capacity under static or dynamic conditions, with a 50 mm stroke length and independent control for monotonic or cyclic loading. The system incorporates position feedback encoders for closed-loop displacement control and is compatible with digital image correlation systems for synchronized strain measurement.

Table iii: Specifications of DIC camera (Photron, Tokyo, Japan)

	Low speed camera	**High speed camera**
Maximum image capture rate	75 fps	1,50,000 fps (at maximum resolution) and 2000 fps (at minimum resolution)
Minimum image capture rate	--	50 fps
Resolution	2448×2048 pixels	1280×1024 pixels
Memory Capacity	--	17,500 images at maximum resolution

Digital Image Correlation (DIC): It is a non-contact optical technique for measuring strain, deformation, and vibration by tracking surface patterns across sequential images. It provides both in-plane and out-of-plane displacement data with high spatial resolution. In this study, DIC was used to measure angular deflection and strain distribution along the compliant articulation segment. The specifications of the DIC camera are listed in Table iii.

1.3. Articulation Experiments

The test setup was mounted on the planar biaxial system, and controlled input displacements were applied to evaluate articulation performance. Two materials, Ti–6Al–4V and Nitinol, were tested to compare deformation behavior and validate the FEA predictions. Based on simulation results, input displacements of 2.2 mm and 5.1 mm were applied at a constant strain rate of 2 mm/min. As displacement increased, the end-effector gradually articulated, reaching its maximum angular deflection at the peak input values (Figure v).

Although the compliant wrist was geometrically designed to accommodate articulation up to approximately 80°–90°, the experimentally validated articulation for the Nitinol prototype was limited to 75° to ensure operation within the conservative super-elastic strain regime.

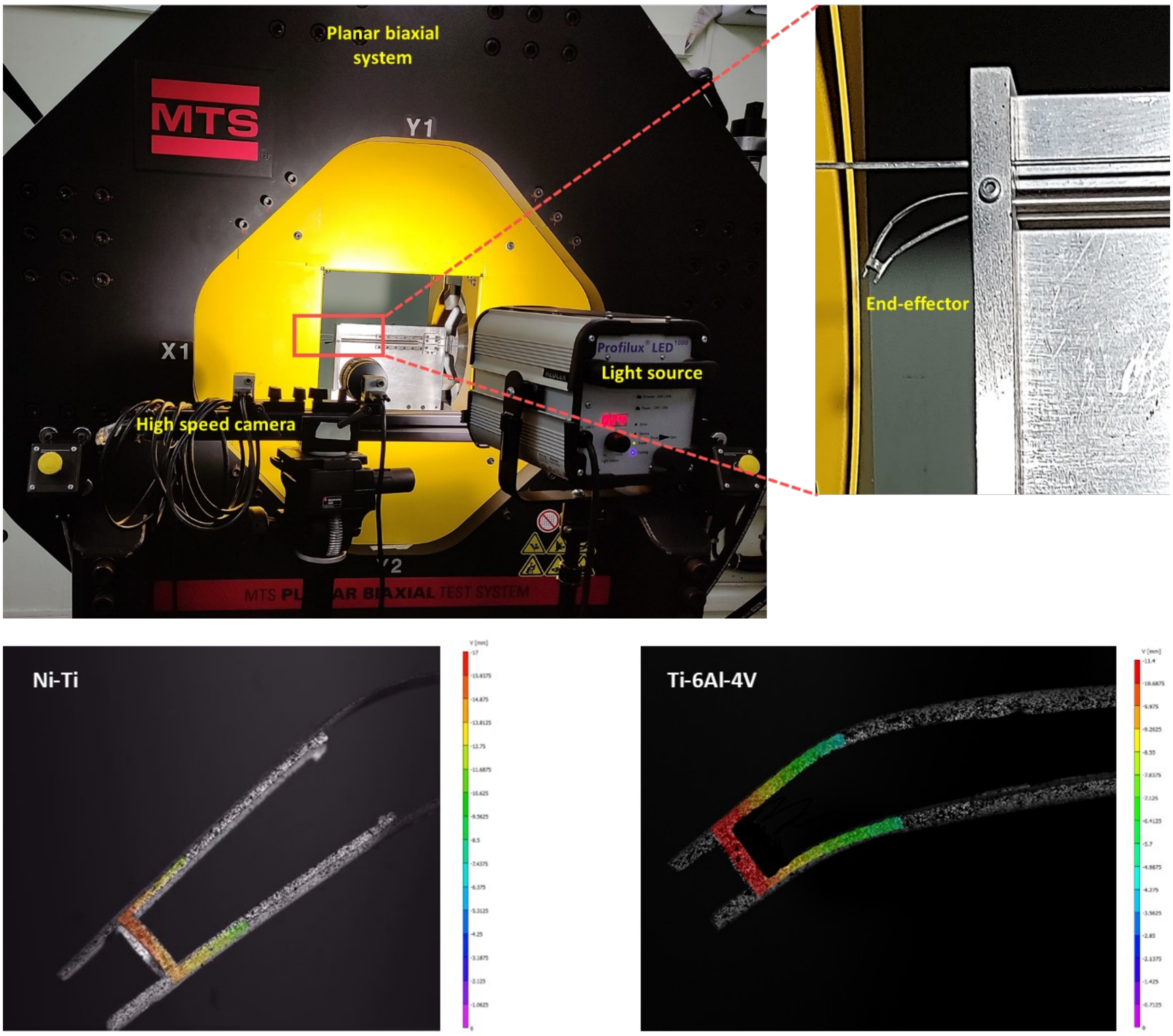

Figure v: Test setup mounted on planar biaxial system and the images of articulating end-effectors captured from DIC camera

3.3.1 Repeatability Assessment

To assess repeatability, each experiment was performed three times for both materials, resulting in a total of six trials. The articulation responses followed consistent trends with limited variation across repetitions. The average deviation was 3.65% for Nitinol and 2.64% for

Ti–6Al–4V (Figure vi (a) and (b)). These values indicate repeatable articulation behavior under the applied loading conditions (Table iv (a)).

3.3.2 *Loading–Unloading Behavior*

To evaluate elastic reversibility, loading–unloading experiments were conducted in which the mechanism was displaced to the maximum input and subsequently returned to zero displacement. This experiment was repeated for both materials. It was observed that the deviation was 0.015 mm for Nitinol and 0.04 mm for Ti-6Al-4V (Figure vi (c) and (d)).

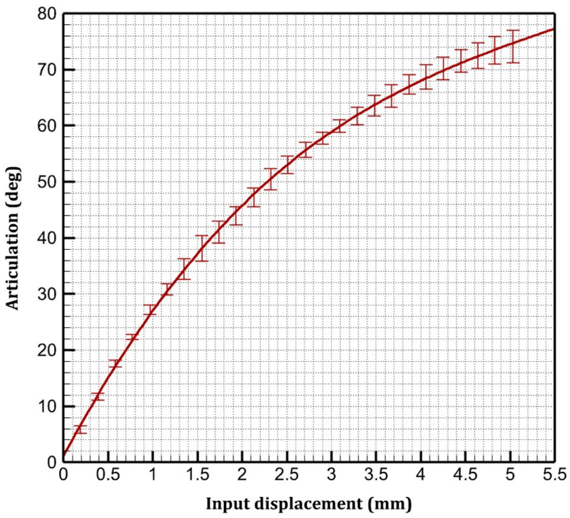

(a)

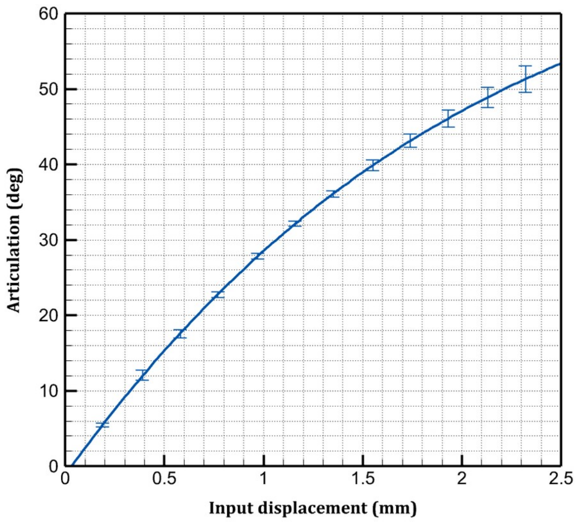

(b)

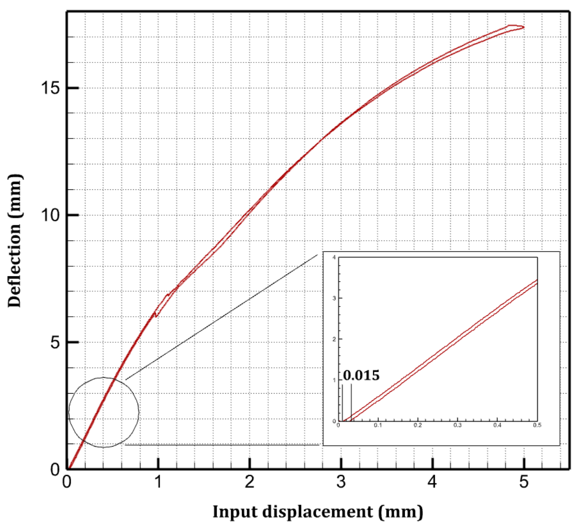

(c)

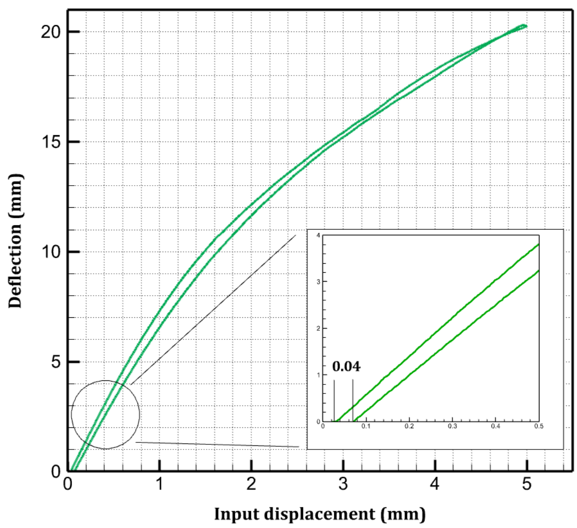

(d)

Figure vi:Experimental results showing repeatability for: (a) Nitinol, (b) Ti-6Al-4V material, Loading and unloading experiment results for: (c) Nitinol, (d) Ti-6Al-4V material

Table iv: Experimental results for variation of articulation

(a) Experiments for repeatability				
Material	**Std. Dev. (deg)**	**Std. Dev. (%)**	**Max. (deg)**	**Max. (%)**

Nitinol	1.59	3.65	2.89	3.91
Ti-6Al-4V	0.75	2.64	1.74	3.39
(b) Variation of articulation with Input Force				
	Mean Error	**Max. Force (N)**	**Max. Articulation**	**Fitted Curve (y =)**
Nitinol	6.47 %	28	75°	$-0.02x^2+3.44x-1.12$
Ti-6Al-4V	7.32 %	36	48°	$-0.03x^2+2.38x-2.23$

3.3.3 Input Force Characterization

The input force required to achieve articulation was measured experimentally and compared with FEA predictions. Figure vii presents the articulation angle as a function of input force for both materials, enabling a direct quantitative comparison between simulated and experimentally measured responses. The results show close agreement across the full articulation range. The maximum actuation force was 36 N for Ti–6Al–4V and 28 N for Nitinol, while the mean difference between experimental and simulated responses was 6.47% for Nitinol and 7.32% for Ti–6Al–4V (Table iv (b)).

The nonlinear FEA analysis also provides insight into the internal mechanical state of the compliant segment during large-deflection articulation. Simulation results indicate that the peak strain remains within the recoverable super-elastic range (□ ≤ 8%) of Nitinol throughout the experimentally validated articulation envelope of 0°–75°.

Furthermore, structural analysis of the gripper assembly under representative peak surgical loading (15 N) indicates that the maximum von Mises stress remains well below the yield strength of the structural materials (SS316L and tungsten carbide). These results confirm that the mechanism maintains adequate structural safety margins under the tested loading conditions, with material strain limits rather than structural yielding acting as the primary design constraint for maximum articulation.

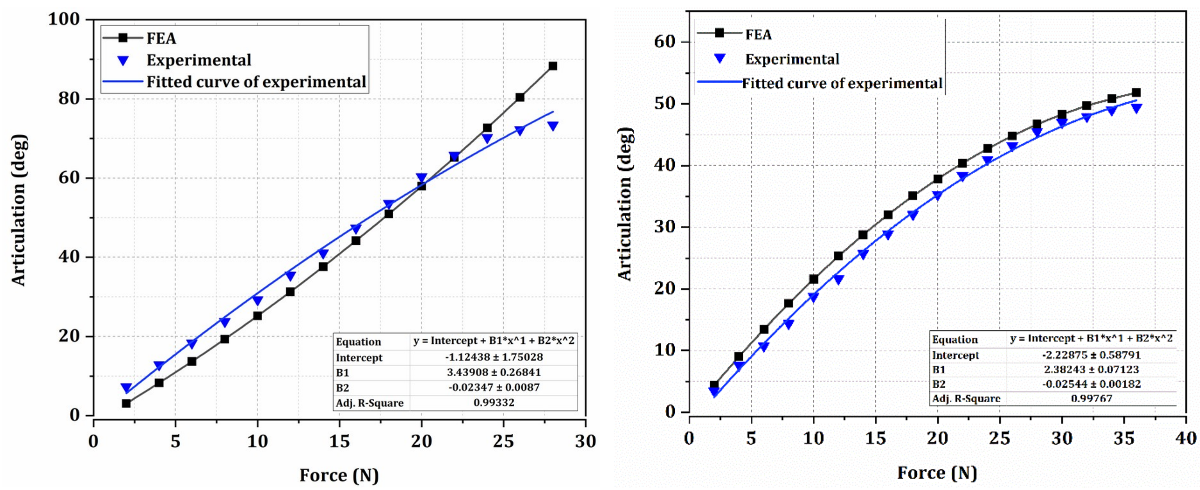

(a) *(b)*

Figure vii: Comparison of input force versus articulation for different models of: (a) Nitinol, (b) Ti-6Al-4V material

A small offset was observed in the experimental force–articulation curves, where force did not return fully to zero upon unloading. This behavior is attributed to residual strain effects and phase transformation characteristics of Nitinol, as well as differences between experimental boundary conditions and modeling assumptions [19].

1.4. Experiments for Gripping Strength Measurement

To evaluate the force-transmission capability of the designed grasper, a series of experiments were performed to measure gripping strength and validate that linkage displacements were consistently translated into tip forces across the full range of jaw angles. Two complementary validation approaches were adopted. In the first method, a force-sensitive resistor (FSR)-based sensor was positioned between the jaws to directly measure contact forces at varying tendon displacements. In the second method, soft silicone models (mechanical analogs of biological tissue) were grasped and pulled to simulate realistic tissue handling, and the transmitted force was recorded via the integrated sensor. Both methods were used to verify that the measured gripping forces matched the predicted mechanical response of the linkage.

Experiments were conducted under quasi-static loading conditions, with applied loads up to 15 N, representing a conservative upper bound exceeding typical laparoscopic manipulation force (generally reported in the 2–10 N range). This controlled framework enables consistent evaluation of gripping force transmission and articulation-dependent performance while minimizing variability introduced by biological tissue viscoelasticity.

3.1.1 Force-Sensitive Resistor (FSR) Sensor

SingleTact capacitive force sensors (PPS UK Ltd., Glasgow, UK) with a measurement range of 10–45 N were used. These sensors were selected for their thin profile (0.35 mm) and reported repeatability errors below 1%. Sensors were interfaced with an Arduino UNO microcontroller and calibrated prior to testing.

3.1.2 Test Setup Design and its Fabrication

The instrument was mounted on a custom test setup designed for gripping force measurement. The setup was modeled in SOLIDWORKS and fabricated using aluminum structural components and 3D-printed pulleys. Grasper actuation was achieved using a stepper-motor-driven screw pulley (NEMA-17, 0.55 N·m), controlled via an Arduino UNO. This configuration enabled controlled, repeatable jaw actuation (Figure viii).

The integrated instrument achieved a maximum gripping force of 13.2 ± 0.47 N at the neutral articulation position. As articulation increased, a gradual reduction in gripping force was observed, with a total decrease of approximately 1.5 N (~11%) across the tested articulation range (Figure ix(c)). This corresponds to a transmission-efficiency parameter of approximately η=0.89 at the maximum tested articulation angle. According to the force-transmission framework presented in Section 2.2.1, articulation-dependent reductions in gripping force are represented through the efficiency parameter η. The observed reduction in η with increasing articulation indicates increasing force-transmission losses associated with tendon routing curvature and contact interactions within the tendon-guiding pathway. These observations are consistent with the expected behavior of tendon-driven mechanisms, where increased routing curvature can reduce the effective transmission of tendon force to the distal end-effector.

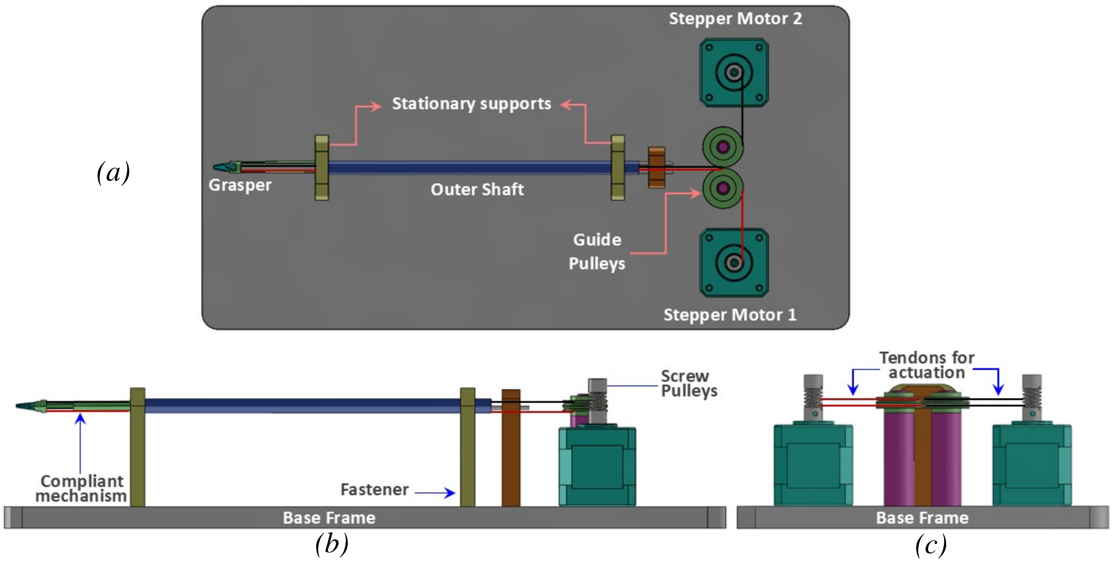

Figure viii:Test setup design showing (a) The top view, (b) Tethers used for actuation, and (c) Fasteners and screw pulleys

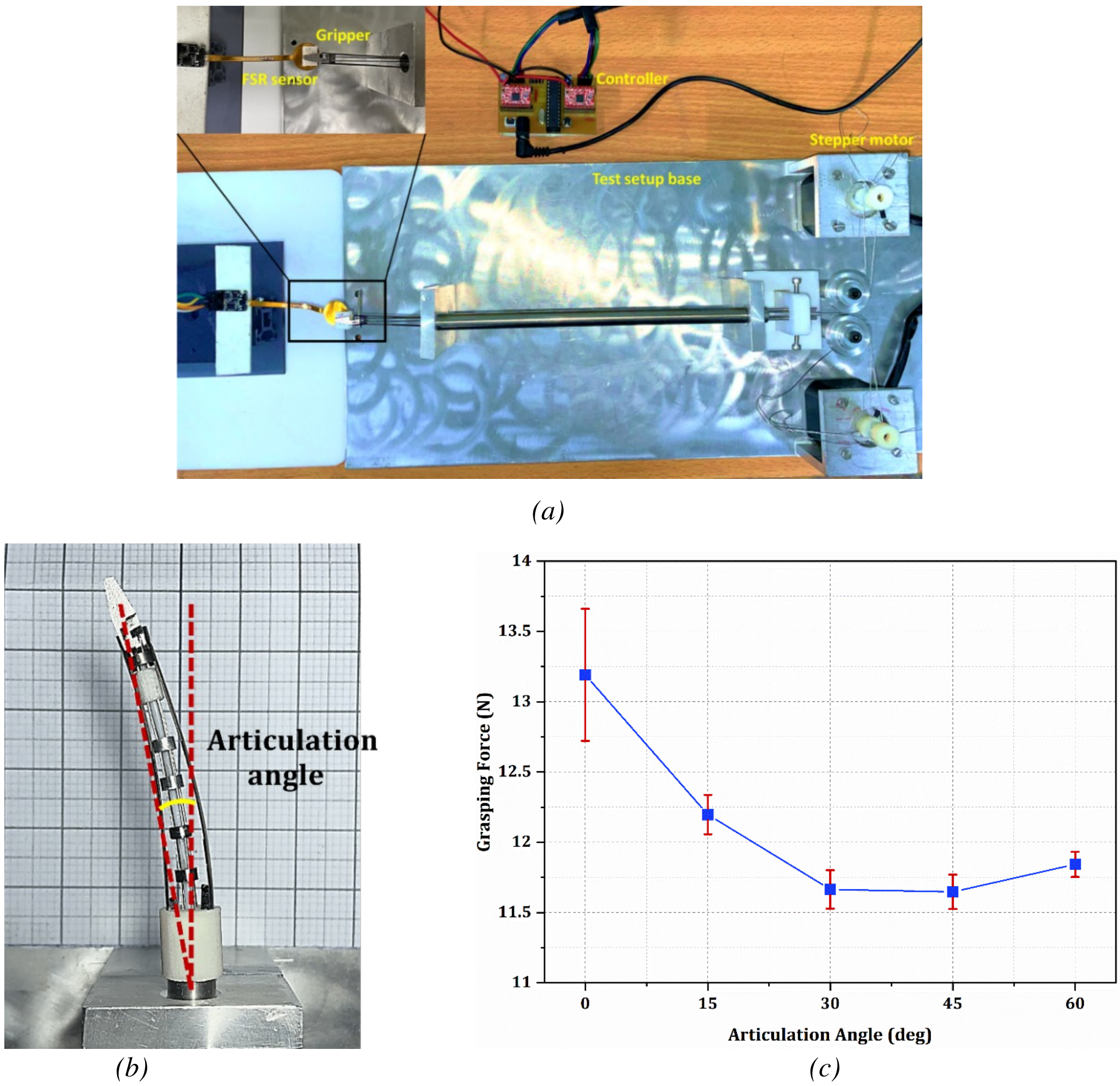

Figure ix:(a) Experimental setup for grasping strength measurement, (b) Grasper at articulating position, and (c) Plot of variation of grasping force at different articulation angles

1.5. Experiments for Pull-Out Strength Measurement

Pull-out strength experiments were performed to evaluate the ability of the grasper to securely retain soft-tissue analogs under tensile loading. Four silicone polymers of varying Shore hardness (Smooth-On Inc., Pennsylvania, USA) were cast into 3-mm-thick test specimens to mimic different soft tissue stiffness levels (Figure x (b)). During each trial, the specimen was grasped at the grasper's maximum gripping force, and pull-out force was measured as the specimen was displaced axially using an inline force sensor (Figure x (a)). The results demonstrated a clear trend: pull-out force increased with increasing material hardness (Figure x (c)), consistent with expected mechanical behavior of stiffer soft-tissue analogs. These results indicate that the grasper maintains effective retention of soft-material analogs across a range of tested stiffness levels.

(a)

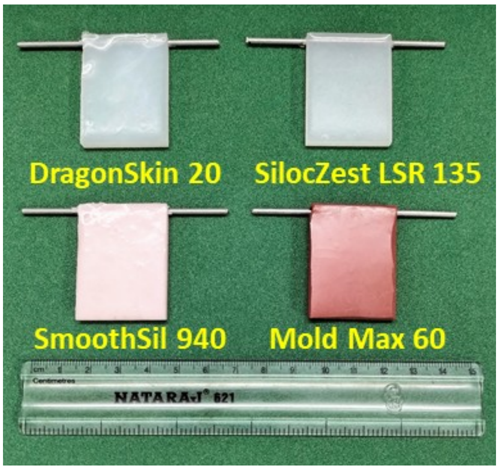

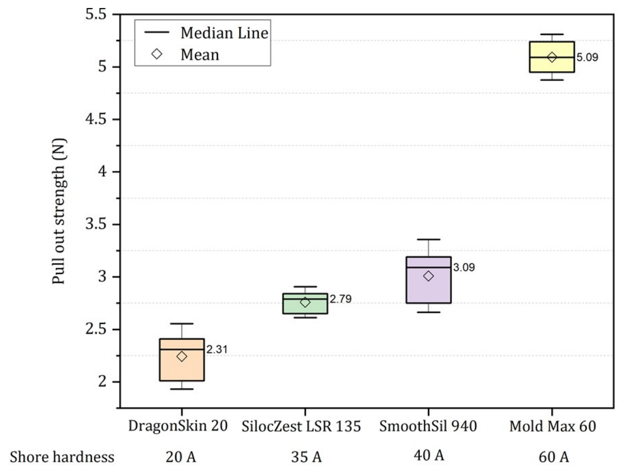

(b) *(c)*

Figure x:(a) Test setup for pull-out strength measurement (b) Test specimens fabricated in Silicone polymers, and (b) Pull-out strength with different specimens

To further characterize the functional safety of the grasper, the damage–slip ratio was evaluated. Defined as the maximum permissible pinch force divided by the minimum pinch force required to prevent tissue slip [20], this ratio serves as an objective measure of jaw performance. A higher ratio indicates a larger safety margin for grasping without tissue trauma.

The ribbed jaw geometry of the proposed grasper resulted in a measured damage–slip ratio of nine. Pull-out force measurements obtained using silicone tissue analogs of varying Shore hardness are shown in Figure x(c). The integrated grasper achieved a maximum gripping force of 13.2 ± 0.47 N at neutral (0°) articulation. Across increasing articulation angles, gripping force decreased modestly but remained within a narrow range. Repeated trials demonstrated low variability, indicating stable and repeatable gripping performance under the tested conditions.

4. DISCUSSION

The present study demonstrates the feasibility of a hybrid compliant–tendon laparoscopic instrument capable of providing articulated distal motion and active grasping within a compact 5 mm form factor. Such capability is particularly relevant for minimally invasive and robot-assisted surgical procedures, where limited instrument dexterity restricts the ability to perform complex tasks in confined anatomical spaces.

The proposed design introduces a functional separation between articulation and force transmission, enabling large-angle deflection without discrete joints while maintaining sufficient gripping force through a tendon–pulley mechanism. This architecture reduces mechanical complexity compared with conventional rigid-link or motor-driven systems, while preserving the dexterity required for surgical manipulation.

Experimental validation demonstrated reliable articulation performance, with strong agreement between FEA predictions and measured behavior. The compliant segment achieved articulation up to approximately 75° while maintaining operation within the super-elastic strain regime of Nitinol. The observed repeatability and minimal hysteresis indicate stable and predictable behavior, which is essential for controlled surgical manipulation.

Grasping experiments showed that the instrument can generate gripping forces of up to 13.2 ± 0.47 N, which are comparable to force levels reported for laparoscopic tissue manipulation, while maintaining consistent performance across articulation angles. The observed reduction in gripping force (~11%) with increasing articulation is attributed to frictional losses along the tendon routing path. While such losses are common in tendon-driven systems, the overall transmission efficiency remained sufficient for practical use.

In addition, the proposed mechanism demonstrated an experimentally measured transmission efficiency of approximately 89% at maximum tested articulation, indicating that the majority of tendon input force is preserved despite articulation-induced routing losses. While these approaches provide excellent dexterity, they often require highly complex assemblies with dozens of moving parts. As detailed in the quantitative benchmarking presented in Table v, existing devices exhibit a fundamental trade-off. Rigid-body systems achieve high grasping forces but suffer from high mechanical complexity. Conversely, fully compliant systems offer low complexity but struggle to integrate high-force grasping. The proposed hybrid design is benchmarked against these systems to demonstrate a balanced optimization: achieving a measured gripping force of 13.2 N and a transmission efficiency of approximately 89% while maintaining substantially lower mechanical complexity than multi-link articulated wrists.

The contribution of the present work is therefore primarily an engineering integration and validation effort, demonstrating that previously established compliant articulation and tendon-driven actuation concepts can be combined within a 5 mm laparoscopic instrument while maintaining functional grasping capability. The accompanying experimental validation provides quantitative evidence of articulation performance, force transmission, and structural feasibility of the integrated design.

Table v: Comparison of the proposed mechanism with representative articulated and compliant surgical instruments.

Device / System	**Mechanism Type**	**Maximum Articulation Angle**	**Maximum Grasping Force**	**Mechanical Architecture / Complexity**	**Experimental Validation**
EndoWrist (Intuitive Surgical)	Cable and Pulley based Articulating (CPA) mechanism	~90° pitch and yaw	Reported load-bearing grasping capability	Multiple discrete links, pulleys, tendons, and joints	Clinical use / commercial system
ArtiSential (LivsMed)	CPA mechanism	>90°	NR	Multi-joint wrist mechanism	Commercial system
FlexDex Surgical	CPA mechanism	~90°	NR	Complex proximal-to-distal mapping	Commercial system
RealHand (Novare Surgical)	Rigid-Body-based Articulating Mechanisms	~80°–90°	Lower mechanical advantage reported	Multiple pivot joints and linkage transmission	Commercial system
Monolithic Compliant Wrist [10]	Compliant mechanism	90°	Not integrated	Monolithic compliant structure	PoC validation
Proposed Design	Hybrid compliant–tendon mechanism	75°	13.2 ± 0.47 N	Compliant wrist + tendon–pulley gripper	FEA, DIC verification, experimental validation

From a practical perspective, the prototype demonstrates that compliant articulation and tendon-based grasping can be combined in a manufacturable design compatible with standard laparoscopic constraints. Although the prototype utilized a simplified material configuration for fabrication, the structural analysis confirmed adequate safety margins under representative surgical loads.

The durability of the compliant segment is governed by its ability to sustain repeated large-deflection cycles within the recoverable strain regime of the material. Experimental loading–unloading tests showed minimal residual deformation (≈ 0.015 mm for the Nitinol prototype), indicating highly elastic and repeatable behavior under the tested conditions. Furthermore, nonlinear FEA predicts peak surface strains below approximately 6.8%, which remain within the super-elastic strain range of Nitinol (typically up to ~8%). Prior studies have shown that fatigue resistance of super-elastic Nitinol is strongly correlated with strain amplitude, with significantly improved cycle life when strains are maintained below the upper transformation limits [21]. Accordingly, the current design was intentionally configured to operate within this strain-bounded regime. While the observed elastic recovery and strain levels are encouraging indicators of durability, comprehensive cyclic fatigue testing remains necessary to establish the long-term fatigue life and operational limits of the instrument.

Some limitations suggest directions for continued engineering development. The evaluation was performed under controlled benchtop conditions using mechanical and soft-tissue analogs and therefore does not fully capture the complexity of in-vivo surgical environments. In addition, the current work focuses on mechanical feasibility and does not include ergonomic assessment or integration into a complete surgical system. The current experimental validation was limited to planar articulation of the compliant segment. Although the architecture permits articulation in different spatial orientations through shaft rotation, independent multi-axis articulation and coupled three-dimensional motion were not experimentally evaluated. Such investigations constitute an important direction for future work.

Future work will focus on improving tendon routing efficiency, optimizing jaw geometry for tissue interaction, and evaluating the device under more realistic surgical conditions. Integration with robot-assisted platforms or advanced handheld systems represents a promising direction for further development.

In conclusion, the proposed hybrid compliant–tendon mechanism provides a compact and low-complexity solution for achieving combined articulation and grasping in minimally invasive surgical instruments. The demonstrated performance supports the feasibility of integrating compliant articulation and tendon-based grasping within compact surgical instruments and provides a foundation for future studies involving advanced surgical tasks and system-level validation.

Acknowledgments

The authors express their sincere gratitude to Dr. Rupesh Ghyar, Biomedical Engineering & Technology Innovation Center (BETIC), Department of Mechanical Engineering, Indian Institute of Technology Bombay, for his valuable technical inputs and continuous support during the development process. The authors also gratefully acknowledge Dr. Amir Hamza Siddiqui and the Advanced Mechanical Testing Facility (AMTF), Indian Institute of Technology Bombay, for their assistance and support in conducting the Digital Image Correlation (DIC)-based experimental measurements. This work was conducted at BETIC, IIT Bombay, with support from the RG S&T Commission, Mumbai, and the Department of Science & Technology, New Delhi.

REFERENCES

[1] R. H. Taylor and D. Stoianovici, “Medical Robotics in Computer-Integrated Surgery,” Oct. 2003. doi: 10.1109/TRA.2003.817058.

[2] P. L. Anderson, R. A. Lathrop, and R. J. Webster, “Robot-like dexterity without computers and motors: a review of hand-held laparoscopic instruments with wrist-like tip articulation,” Jul. 02, 2016, *Taylor and Francis Ltd*. doi: 10.1586/17434440.2016.1146585.

[3] P. Kumar and B. Ravi, “A comparative study of robots in laparoscopic surgeries,” in *ACM International Conference Proceeding Series*, Association for Computing Machinery, Jul. 2019. doi: 10.1145/3352593.3352608.

[4] P. Kumar, S. Talele, S. Deshpande, R. Ghyar, S. Rout, and B. Ravi, “Design, Analysis and Experimental Validation of a Novel 7-Degrees of Freedom Instrument for Laparoscopic Surgeries,” *Ann. Biomed. Eng.*, vol. 51, no. 4, pp. 751–770, Apr. 2023, doi: 10.1007/s10439-022-03086-w.

[5] C. Freschi, V. Ferrari, F. Melfi, M. Ferrari, F. Mosca, and A. Cuschieri, “Technical review of the da Vinci surgical telemanipulator,” 2013, *John Wiley and Sons Ltd*. doi: 10.1002/rcs.1468.

[6] S. F. Hardon, F. Schilder, J. Bonjer, J. Dankelman, and T. Horeman, “A new modular mechanism that allows full detachability and cleaning of steerable laparoscopic instruments,” *Surg. Endosc.*, vol. 33, no. 10, pp. 3484–3493, Oct. 2019, doi: 10.1007/s00464-019-06849-0.

[7] J. W. Klok, R. Postema, A. T. Steinporsson, J. Dankelman, and T. Horeman, “Design and Evaluation of a Balanced Compliant Laparoscopic Grasper,” *IEEE J. Transl. Eng. Health Med.*, vol. 11, pp. 451–459, 2023, doi: 10.1109/JTEHM.2023.3291925.

[8] B. Zhu *et al.*, “Design of compliant mechanisms using continuum topology optimization: A review,” Jan. 01, 2020, *Elsevier Ltd*. doi: 10.1016/j.mechmachtheory.2019.103622.

[9] K. Chandrasekaran and A. Thondiyath, “Design of a tether-driven minimally invasive robotic surgical tool with decoupled degree-of-freedom wrist,” *International Journal of Medical Robotics and Computer Assisted Surgery*, vol. 16, no. 3, Jun. 2020, doi: 10.1002/rcs.2084.

[10] T. L. Thomas, V. K. Venkiteswaran, G. K. Ananthasuresh, and S. Misra, “A Monolithic Compliant Continuum Manipulator: A Proof-of-Concept Study,” *J. Mech. Robot.*, vol. 12, no. 6, Dec. 2020, doi: 10.1115/1.4046838.

[11] H. G. Le, N. L. Ho, and T. P. Dao, “Design synthesis, modeling, control strategies, and fabrication methods of compliant grippers for micromanipulation and micromanipulator: A comprehensive review,” Apr. 01, 2025, *Elsevier Ltd*. doi: 10.1016/j.rcim.2024.102893.

[12] Y. A. AboZaid, M. T. Aboelrayat, I. S. Fahim, and A. G. Radwan, “Soft robotic grippers: A review on technologies, materials, and applications,” Jul. 01, 2024, *Elsevier B.V.* doi: 10.1016/j.sna.2024.115380.

[13] H. Llewellyn-Evans, C. A. Griffiths, and A. Fahmy, “Microgripper design and evaluation for automated μ-wire assembly: a survey,” Jun. 01, 2020, *Springer*. doi: 10.1007/s00542-019-

04741-4.

[14] P. Kumar and B. Ravi, "Design optimization and multi-method analysis of a novel compliant mechanism-based articulated laparoscopy instrument," *Next Research*, vol. 2, no. 3, p. 100668, Sep. 2025, doi: 10.1016/j.nexres.2025.100668.

[15] A. Hackethal, M. Koppan, K. Eskef, and H. R. Tinneberg, "Handheld articulating laparoscopic instruments driven by robotic technology. First clinical experience in gynecological surgery," *Gynecol. Surg.*, vol. 9, no. 2, pp. 203–206, May 2012, doi: 10.1007/s10397-011-0708-2.

[16] P. Kumar *et al.*, "Surgeon perception of factors affecting the efficiency of conventional and robotic laparoscopy: A Pan India study," *Heliyon*, vol. 8, no. 12, Dec. 2022, doi: 10.1016/j.heliyon.2022.e12561.

[17] J. E. Shigley, C. R. Mischke, and R. G. Budynas, *Mechanical Engineering Design*, 10th ed. New York: McGraw-Hill Education, 2015.

[18] M. Chavan, P. Kumar, R. Ghyar, B. Ravi, and P. S. Gandhi, "Tendon-Driven Detachable End-Effector Mechanism for Minimally Invasive Surgery (MIS) Instruments," in *Smart Innovation, Systems and Technologies*, Springer Science and Business Media Deutschland GmbH, 2021, pp. 619–628. doi: 10.1007/978-981-16-0084-5_51.

[19] D. J. Siddons and J. R. Moon, "Tensile and compression performance of superelastic NiTi tubing," *Materials Science and Technology*, vol. 17, no. 9, pp. 1073–1078, 2001, doi: 10.1179/026708301101511202.

[20] E. A. M. Heijnsdijk, H. DeVisser, J. Dankelman, and D. J. Gouma, "Slip and damage properties of jaws of laparoscopic graspers," *Surgical Endoscopy and Other Interventional Techniques*, vol. 18, no. 6, pp. 974–979, Jun. 2004, doi: 10.1007/s00464-003-9153-2.

[21] A. R. Pelton, "Nitinol fatigue: A review of microstructures and mechanisms," in *Journal of Materials Engineering and Performance*, Jul. 2011, pp. 613–617. doi: 10.1007/s11665-011-9864-9.